THE INFLUENCE OF DEPOSITION CONDITIONS ON THE NANOHARDNESS AND SCRATCH BEHAVIOR OF THIN DC MAGNETRON SPUTTERED CrN COATINGS

P. Hviščová, F. Lofaj, M. Novák

Abstract

The influence of total gas pressure, nitrogen content and substrate bias on nanohardness and scratch behavior has been investigated on DC magnetron sputtered CrN coatings deposited on steel substrates. The nanohardness of the coatings increased with the increase of N_2 content and the highest nanohardness of ~22 GPa was reached at 50 vol.% of nitrogen with a floating bias. Compressive stresses up to 3.6 GPa were generated in the coatings. They affected both nanohardness and scratch behavior. The maximum critical loads L_{c1} during scratch testing were in the range 150 ÷ 204 mN. The critical loads were strongly influenced by the intrinsic residual stresses which were considerably larger than thermal stresses. The compressive residual stresses contributed to the increase of coating nanohardness and simultaneously decreased critical loads and caused delamination. However, nitride formation contributed to the nanohardness increase more significantly than the residual stresses.

Keywords: CrN coatings, nanohardness, scratch test, DC magnetron sputtering, nitrogen content

INTRODUCTION

Chromium nitride coatings obtained by DC magnetron sputtering exhibit relatively favorable mechanical properties combined with high corrosion resistance. However, properties of these nitrides strongly depend on the deposition conditions. Different Cr–N phases can be obtained in dependence on the amount of nitrogen, starting from Cr, Cr+N, Cr+N+Cr_2N, CrN_x up to CrN [1-5]. The hardness of chromium nitride coatings, which is usually in the range 22 – 25 GPa, depends also on the nitrogen content added during reactive magnetron sputtering. Besides hardness, adhesion of the coating to the substrate is among the critical parameters for its practical applications.

Scratch testing is a standardized method for the measurement of the adhesion between the substrate and the coatings. During testing, diamond stylus scratches the surface of the coating with a constant speed with a gradually increased (or constant) load. The values of L_c measured after the scratch testing (see Fig.1) correspond to critical loads at which different types of coating failure occur [3].

The critical load L_{c1} is the load at which the first cracks appear in the coating. The load L_{c2} leads to substantial damage of the coating and its local delamination from the substrate. The load, at which the coating is peeling off, is denoted as L_{c3}. Damage to the

Petra Hviščová, František Lofaj, Michal Novák, Institute of Materials Research of the Slovak Academy of Sciences, Watsonova 47, Košice, Slovakia
František Lofaj, Michal Novák, Faculty of Materials Science and Technology, Slovak University of Technology, Bottova 25, Trnava, Slovakia

coating can be divided into two groups: cohesive failure which is caused by tensile stress that arises behind the stylus and result in so-called “through – thickness” cracking. The second group attributed to the adhesive failure is caused by the compressive stresses in front of the stylus tip. These adhesive failures occur as cracking and buckling of coating or by full separation of the coating from the substrate (spallation and chipping) [6]. The corresponding critical loads depend on several factors: adhesion of the coating to the substrate, stylus radius, loading rate, mechanical properties of coating and substrate, coating thickness, residual stresses in the coating and friction between coating and stylus. Zhang, et al. [7] prepared Cr and CrN coatings by twin target median frequency magnetron sputtering with various nitrogen contents and investigated microstructure, electrical resistivity and coefficient of friction as a function of N_2 content. They found that CrN forms only when the amount of nitrogen is sufficient, while Cr and Cr_2N phases form at lower amounts of nitrogen. They measured the critical load L_{c1} ~225 mN in Cr coatings; in CrN_x coatings, critical load was ~137 mN. After scratch testing, in the case of low N_2 content when only Cr phase was present, no cracks appeared and it failed due to discontinuous chip removal. Such behavior corresponds to ductile behavior and the excellent adhesion of pure Cr to steel. On the other hand, scratches in CrN_x coatings showed an abrupt delamination by flaking resulting from high brittleness and poor adhesion of the coating to the substrate [7]. However, the scratch behavior in this work has not been correlated with the hardness of the coatings.

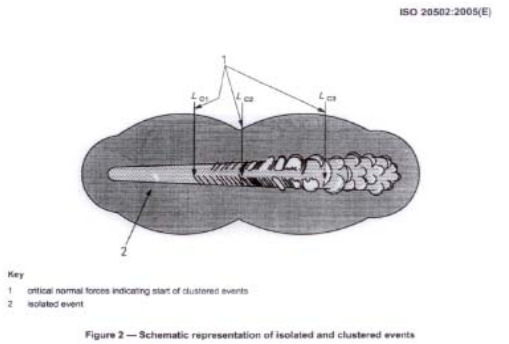

Fig.1. Scratch track.

The aim of this work is to determine the influence of total gas pressure, bias and nitrogen content on the nanohardness and critical loads during the scratch testing of conventional DC magnetron sputtered Cr–N coatings.

EXPERIMENTAL PROCEDURE

Twenty nine samples of CrN coatings were deposited on polished construction steel substrate with Ø 25 mm in Cryofox Discovery 500 (Polyteknik, Denmark) using a DC magnetron sputtering from a 75 mm Cr target at a constant power of 700 W. The distance between substrate and target was 7 cm and the deposition time varied from 5 to 30 minutes.

The sputtering was carried out under constant working pressure either in pure Ar atmosphere or in a mixture of Ar and up to 70 vol. % of nitrogen in total gas flow. The effect of nitrogen content was studied at the total pressure of 0.5 Pa. The influence of total gas pressure flow was investigated in the pressure range 0.3 – 0.7 Pa with 20 vol. % of N_2. Negative DC bias was studied in the range 30 – 300 V at 0.4 ÷ 0.6 Pa total pressure and 50 vol. % of nitrogen.

The thickness of the coatings was measured by confocal microscope (Plu neox, Sensofar – Tech, S.L., Spain) at three different locations with sharp edges. The deposition

rate was calculated from the ratio between the coatings` thickness and total deposition time. The nanohardness was measured using nanoindenter (G200, Agilent Technologies, USA) in continuous stiffness measurement mode for thin coatings (CSM for coatings), constant strain rate 0.05 s^{-1}, depth modulated amplitude 2 nm, frequency 45 Hz and up to the constant penetration depth of 600 nm [8, 9]. Scratch tests were performed on the same nanoindenter using a maximum force of 500 mN, sliding rate 100 μms^{-1} and length of 1000 μm. Two scratches were made on each test sample. The scratch paths and cross section were observed using optical, confocal and scanning electron microscopy.

RESULTS AND DISCUSSION

The deposition conditions used for the preparation of Cr–N coatings, are summarized in Tab.1 The measured thickness of the coatings was in the range from ~700 nm to ~2300 nm (Tab.1) in dependence on the time and also on the other deposition parameters.

Tab.1 Deposition parameters, deposition rate and hardness of the studied CrN coatings.

Sample	Gas pressure [Pa]	Content N_2 [vol. %]	Negative bias [V]	Deposition time [min]	Thickness [nm]	Deposition rate [nm/min]	Hardness [GPa]
CrN 70	0.2	20	Floating	5	777 ± 51	155 ± 10	20 ± 1
CrN 69	0.3	20	Floating	5	743 ± 56	149 ± 11	20 ± 1
CrN 23	0.3	20	Floating	5	792 ± 26	158 ± 5	19 ± 1.5
CrN 24	0.4	20	Floating	5	686 ± 14	137 ± 3	21 ± 3
CrN 25	0.5	20	Floating	5	721 ± 22	144 ± 4	21.2 ± 2
CrN 71	0.5	20	Floating	5	825 ± 55	165 ± 11	19 ± 1
CrN 72	0.7	20	Floating	5	709 ± 57	142 ± 11	21.5 ± 1
CrN 73	1.2	20	Floating	5	-	-	17.5 ± 1.5
CrN 28	0.5	70	Floating	30	2337 ± 55	78 ± 2	22 ± 1.8
CrN 29	0.5	60	Floating	16	1362 ± 21	85 ± 1	21.8 ± 2
CrN 30	0.5	50	Floating	13	1462 ± 42	113 ± 3	21.5 ± 2
CrN 31	0.5	40	Floating	7	-	-	13.1 ± 2
CrN 32	0.5	30	Floating	6	827 ± 23	138 ± 4	19.3 ± 1.7
CrN 33	0.5	20	Floating	5	791 ± 49	158 ± 10	15.5 ± 2
CrN 34	0.5	0	Floating	5	755 ± 23	151 ± 5	13.9 ± 1.8
CrN 40	0.5	50	-30	15	1533 ± 59	102 ± 4	18.5 ± 1
CrN 36	0.5	50	- 50	15	1484 ± 42	99 ± 3	18.2 ± 1.9
CrN 41	0.5	50	-60	15	1522 ± 74	102 ± 5	20.5 ± 1.5
CrN 37	0.5	50	-100	15	1104 ± 36	74 ± 2	20.3 ± 2
CrN 38	0.5	50	-200	15	-	-	10.9 ± 1.5
CrN 39	0.5	50	-300	15	-	-	11 ± 2
CrN 46	0.6	50	Floating	15	-	-	21.5 ± 1-5
CrN 47	0.6	50	-30	15	-	-	12.5 ± 1
CrN 48	0.6	50	-50	15	-	-	12 ± 1.5
CrN 49	0.6	50	-60	15	-	-	13 ± 1
CrN 63	0.6	50	-300	15	-	-	28 ± 2
CrN 50	0.4	50	-30	15	1567 ± 57	105 ± 4	22 ± 1.5
CrN 51	0.4	50	-50	15	1434 ± 27	96 ± 2	20 ± 1
CrN 52	0.4	50	-60	15	1743 ± 56	116 ± 4	22.5 ± 2

Figures 2 a,b show the structure of the cross sections of pure Cr coating and CrN coating respectively, which was prepared with 70 vol. % of nitrogen of total gas flow. In both cases, dense fiber structure with a width of grains of several tenths of a micron was observed. X – ray diffraction showed that the coatings are polycrystalline with preferential (111) and (200) orientations [10].

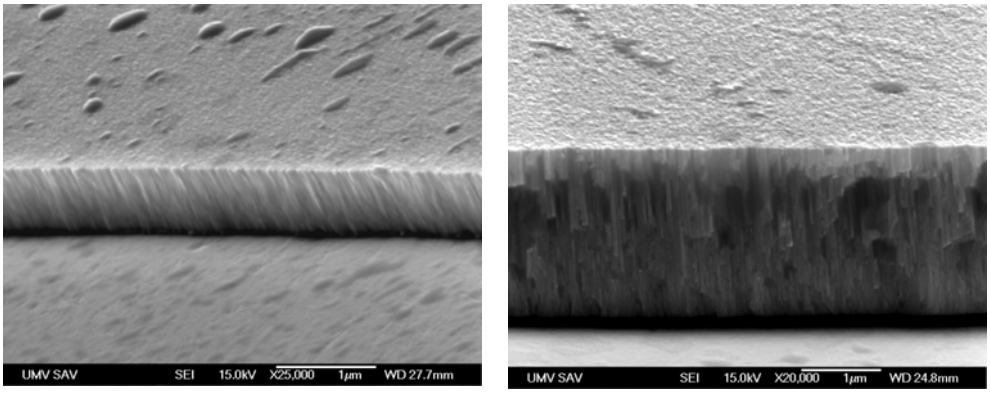

a) b)

Fig.2. Microstructure of a) Cr coating and b) CrN coating prepared with 70 vol. % N_2 of total gas flow.

The deposition rate in the first series of coatings (CrN 70 ÷ CrN 73) did not change markedly with increasing pressure in the deposition chamber. The deposition rate was in the range 137 – 165 nm/min within the pressure range 0.2 Pa – 0.7 Pa. The differences were usually within the scatter of the measurement and the increased Ar ion concentration at the higher pressure seems to be compensated by a larger number of collisions of metal atoms with the gas molecules on their way toward the substrate.

On the other hand, deposition rate was reduced from 144 nm/min to only 78 nm/min when nitrogen content was increased from 20 vol. % to 70 vol. % (see CrN 28 ÷ CrN 34). The reasons for the reduction may be that the nitrogen content increase occured at the expense of Ar. Thus, the concentration of Ar ions, which sputter Cr from the target, decreased and the sputtering rate also had to decrease.

Another explanation may be target poisoning: when nitride formed on the target surface due to an excess of nitrogen, sputtering rate reduction had to occur [11]. These effects, combined with the phase evolution during nitrogen content increase, influenced the measured properties.

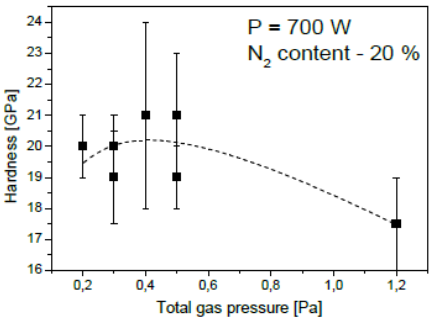

Fig.3. Influence of total gas pressure on Cr–N coatings nanohardness.

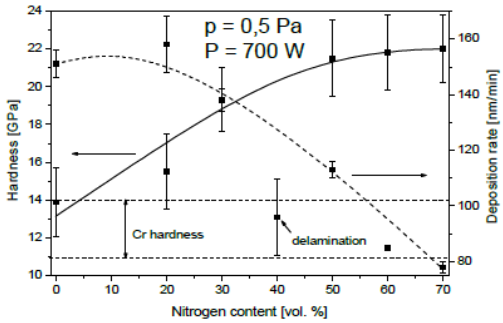

Fig.4. The dependence of nanohardness Cr–N coatings on nitrogen content.

Figure 3 shows the dependence of nanohardness on total gas pressure obtained in the case of the 20 vol.% N_2 addition into the flow of Ar gas. The nanohardness of these coatings was in the range 19 ÷ 21 GPa when prepared in the pressure range 0.4 – 0.6 Pa. Further increase of total gas pressure up to 1.2 Pa led to the reduction of nanohardness to 17 GPa. Fig.4 shows the influence of nitrogen content on Cr–N nanohardness. The nanohardness of pure chromium coatings was in the range 11÷14 GPa. This agrees well with the value of 11.5 GPa reported for bulk Cr [12]. With the addition of up to 50 vol. % nitrogen, the nanohardness gradually rose up to 22 GPa. Further increase of nitrogen content above 50 vol. % had no significant influence on CrN nanohardness and its values remained approximately constant (~22 GPa). The deposition rates and their decrease correlated with nanohardness behavior up to ~50 vol.% but the rate decrease continued up to 70 vol.%, which agrees with the previous arguments.

The behavior shown in Fig.4 may be explained in terms of nanohardness increase due to gradual nitride formation and/or gradual increase of residual stresses. The only exclusion was obtained at 40 vol. % N_2. In the all three samples prepared with 40 vol. % of nitrogen, massive delamination occurred. Obviously, high residual stresses were presented and the nanohardness of the remains of the coating was only ~13 GPa. Our first X-ray measurements of the residual stresses suggested they were compressive around 0.15 GPa in the pure Cr coating and around 3.6 ± 1.1 GPa in CrN 28 coating, respectively [10].

Daniel et al. [13] reported that the value of compressive residual stresses depends on CrN coating thickness. In the case of pure Cr coatings, they were ~1.5 GPa at around 200 nm and they were reduced to 0,3–0,5 GPa at a thicknesses above 1 µm. This is slightly higher than measured in the current case. In the CrN coating, similar behavior has been reported: ~200 nm thin coating, the compressive stresses were more than 2 GPa, and they were reduced to 1.1 – 0.9 GPa at the thickness above 0.9 µm [13]. Although these values are slightly lower than in the studied CrN coatings, they are within the same range. The differences may result from different thicknesses and different substrate temperatures because the substrates were unheated in our case. In W-C coatings, the compressive residual stresses caused an approximately linear increase of the measured nanohardness [14]. However, when the adhesion was not sufficient, compressive stresses above several GPa resulted in extensive cracking and complete delamination in a similar way as was observed in the studied CrN coatings. Thus, the cracking and delamination in Cr–N coatings can also be attributed to the presence of the measured compressive residual stresses. The cracking of CrN coatings results in the relaxation of residual stresses and the elimination of their contribution explains subsequent nanohardness decrease.

The influence of negative DC bias on coating nanohardness is illustrated in Fig 5. Negative bias in the range 30÷100 V resulted in a small decrease of the nanohardness values from 22÷24 GPa with a floating bias to 22 GPa at 0.4÷0.5 Pa, and strong decrease to ~12 GPa at 0.6 Pa. When the negative bias was more than 100 V, strong delamination occurred, presumably due to excessive compressive stresses. Indeed, high bias potential has been reported to cause the decrease of nanohardness due to a decrease of coating crystallinity [15]. The small reduction of nanohardness in the coatings, deposited at the pressure 0.4 and 0.5 Pa with the negative bias below 100 V, is contrary to the results reported by Kim [15]. They found hardness increase, because an increased negative bias shall raise kinetic energy of chromium ions which results in denser structure. The reason for the disagreement among their results and ours is not clear and repeated experiments in the bias range from 0 to 50 V are necessary.

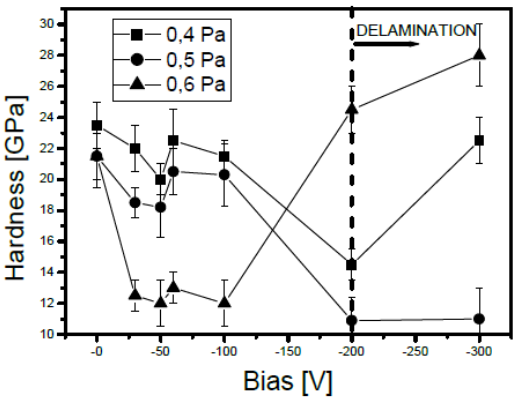

Fig.5. The effect of negative bias on nanohardness of CrN coatings with 50 vol. % of N_2 in total gas flow.

As already mentioned, compressive stresses in the coating affect the measured nanohardness. True nanohardness of the coatings can be obtained when the compressive stress effect is subtracted from the measurement. Additional scratch tests were performed in order to obtain information necessary to separate these effects.

Figure 6 shows the dependence of penetration depth and load along two scratches in the same coating (CrN 54). The first slight oscillations of the curve appeared at around 50 μm distance when the first damage of the coating occurred. It corresponded to L_{c1}. Critical load L_{c2} was reached when significant oscillations at ~250 μm on the scratch curve emerged. The values of L_{c1} and L_{c2} from scratch curves can be directly compared with the scratch topography in Fig.5b. The values of L_{c1} and regular cracking at L_{c2} are indicated there. The comparison reveals good agreement with the values obtained from the scratch curves.

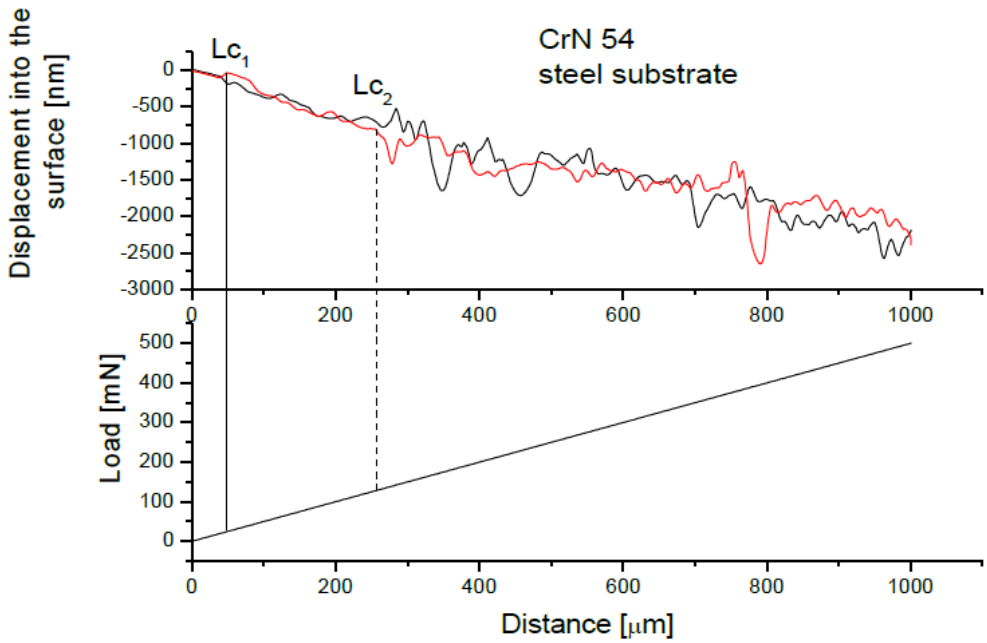

a)

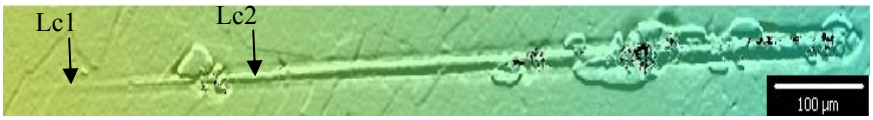

b)

Fig.6. Two scratch curves in CrN 54 coating - a) and the micrograph of one of the scratches with L_{c1} and L_{c2} areas indicated – b).

Figure 7a) shows details of the cracks formed in the scratch during testing in the zone corresponding to L_{c1}. The small cracks along the scratch track are called lateral cracks. These cracks belongs to the group of through-thickness cracks generated by tensile stresses and occur by cohesive failure. Besides lateral cracks, additional cracks with the shape of arcs opening away from the direction of scratching were observed at slightly higher loads. They resemble buckling cracks [16].

Figure7 b) shows arc cracks and occasional buckling spallations observed in the L_{c2} zone. These cracks are similar to buckling cracks, but the wide, arc-shaped patches are missing. Buckling or lifting belong to the adhesive failures, when the coating fully separates from the substrate. This damage commonly occurs under the compressive stresses in front of the indenter [16].

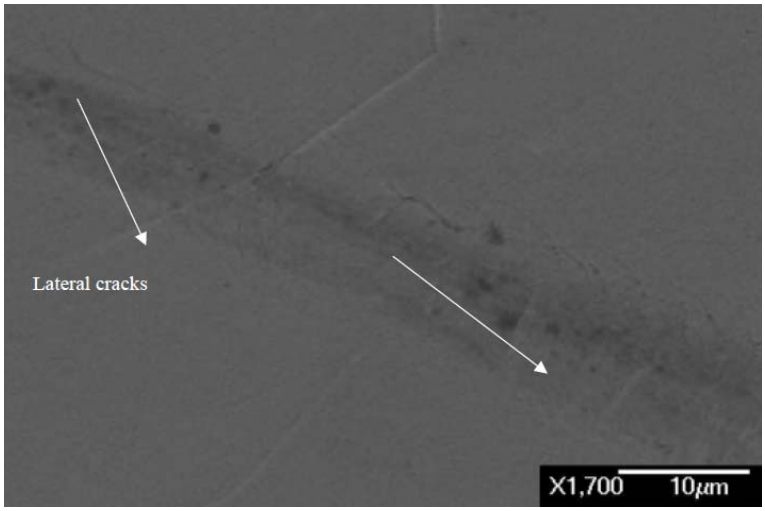

a)

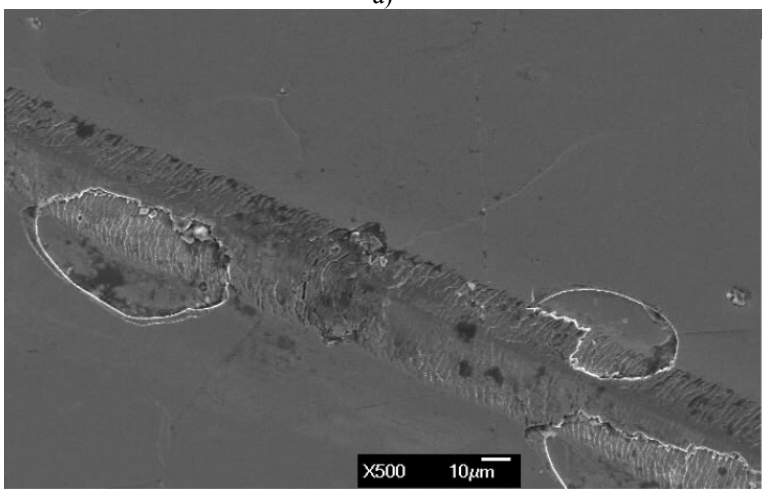

b)

Fig.7. Details of the scratch track in the zone of critical load L_{c1} – a) and critical load L_{c2} –b).

Figure 8 summarizes the effect of total working gas pressure on critical loads. Despite significant scatter, the highest critical loads L_{c1} in the range 150 - 204 mN were measured in the coatings prepared under the pressure 0.4 Pa and 0.5 Pa. The maximum values of L_{c1} of coatings prepared outside this interval were slightly lower. Note that the highest nanohardness was also obtained in the range 0.4 – 0.5 Pa. Interestingly, L_{c2} exhibits smaller scatter and negligible dependence on total pressure.

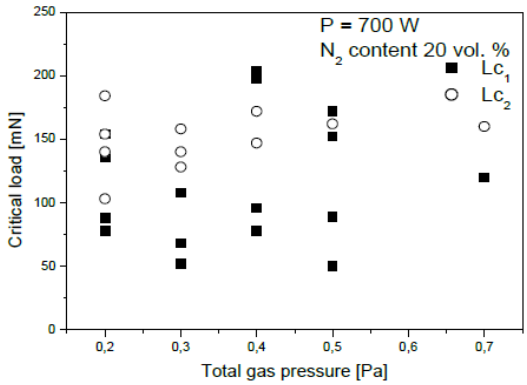

Fig.8. Influence of total gas pressure on critical load in CrN coatings prepared with 20 vol. % of nitrogen content.

Figure 9 illustrates that the critical load L_{c1} may increase up to three times from ~45 mN to ~150 mN when N_2 content increased from 0 vol. % to 20 vol. %. This observation is consistent with the work of Seok [17] who reported a strong increase of critical load when N_2 content increased from 0 to 7%. Further addition of nitrogen resulted in a decrease of critical loads again to 50 mN. On the other side, coating hardness exhibits an opposite trend: it increases with nitrogen content increase (Fig.3). Such behavior can be explained by the effect of compressive residual stresses. Higher residual stresses contribute to higher hardness, while critical loads decrease.

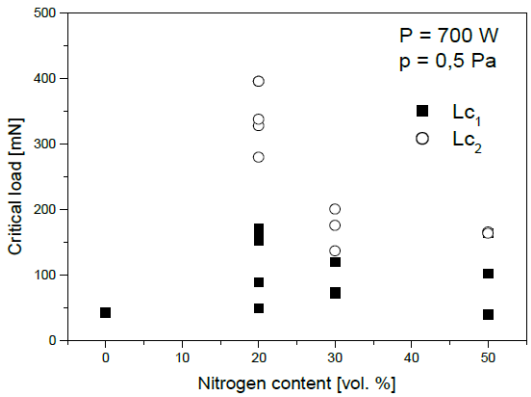

Fig.9. Dependence of critical load on nitrogen content in Cr–N coatings.

Because of the thick steel substrate, residual stresses can be measured only by X-ray diffraction. The measurements performed up to the present are only preliminary and do not provide full dependence. Therefore, an analogy with the results on W – C coatings with known residual stresses is used because the measured stresses are in the same range. The residual stresses σ_r present in the coatings consists of intrinsic (σ_{in}), thermal (σ_{th}) and extrinsic (σ_{ext}) stresses [18]. The extrinsic residual stresses are usually negligible whereas the intrinsic stresses arise from compressive changes on the grain boundaries, diffusion processes and due to impigning particle effects. The stresses due to a different thermal

expansion coefficient of the substrate and coating can be estimated according to the formula [19]:

$$\sigma_{th} = (\alpha_{coat} - \alpha_{sub})\Delta T \frac{E_{coat}}{1-\nu_{coat}}$$

The value of ΔT was estimated to be ~100°C, because the deposition temperature was around 130 °C. For $\alpha_{steel} = 12x10^{-6}$ K^{-1}, $\alpha_{CrN} = 2.3 \times 10^{-6}$ K^{-1}, $E_{CrN} = 200$ GPa and $\nu = 0.2$ [20], the calculation gives σ_{th} ~0.25 GPa. When assuming $\sigma_r = \sigma_{in} + \sigma_{th}$, for the maximum residual stresses in Cr–N coatings $\sigma_r = 3.6 \pm 1.1$ GPa and σ_{th} ~0.25 GPa, the intrinsic residual stresses are absolutely dominant ($\sigma_{in} > 3{,}2$ GPa). However, the measured increase of nanohardness with the increase of nitrogen content is around 8 GPa from 14 GPa to 22 GPa (see Fig.4). Obviously, most of the measured nanohardness increase has to result from the formation of harder CrN phase.

Coating thickness was already shown to be another important factor determining the value of residual stresses. It was shown on Cr–N and W – C coatings [13,14] that their value rapidly drops with the increase of the coatings` thickness until a certain approximately constant value is reached at the thicknesses around 1 μm depending on the coating composition and deposition conditions. Current Cr–N coatings fall just in the range of transition from high and compressive residual stresses to relatively low and stable stresses in the case of thicker coatings. Thickness variations resulting in stress variations in the coatings prepared under similar conditions could explain the variation of Lc_1 observed in Fig.8 and Fig.9. However, additional direct measurement of residual stresses on well-defined coatings are necessary to determine this correlation quantitatively.

Thus, the effect of intrinsic residual stresses on nanohardness and scratch behavior is not straightforward and depends on a number of factors besides total pressure, nitrogen content and bias. Generally, the role of residual stresses is more detrimental than beneficial, because the possible nanohardness increase does not compensate for coating delamination.

CONCLUSION

The total gas pressure does not affect the deposition rate of Cr–N significantly, while the increase of nitrogen content reduces deposition rate almost in half. The optimum pressure for deposition of relatively hard Cr–N coatings is in the range 0.4 – 0.6 Pa. The addition of nitrogen up to 50 vol. % results in the increase of the coatings` nanohardness by creating harder CrN coatings, which is accompanied by a generation of compressive residual stresses up to 3,6 GPa. These stresses cause a decrease of critical loads during scratch testing. The residual stresses are dominated mostly by the intrinsic residual stresses. It can be concluded that although the residual stresses in the coating exhibit a positive effect on nanohardness, they simultaneously reduce critical loads and result in delamination of coatings. The observed nanohardness increase results mostly from the formation of harder nitride phase and the residual stresses constitute a minor contribution.

REFERENCES

[1] Barata, A., Cunha, L., Moura, C.: Thin Solid Films, vol. 398-399, 2001, p. 501
[2] Hoy, R., Kammainga, JD., Janssen, GCAM.: Surface and Coatings Technology, vol. 200, 2006, p. 3856
[3] Van Essen, P., Hoy, R., Kamminga, JD., Ehiasarian, AP., Janssen, GCAM.: Surface and Coatings Technology, vol. 200, 2006, p. 3496
[4] Lee, JW., Tien, SK., Kuo, YCh.: Thin Solid Films, vol. 494, 2006, p. 161
[5] Fornies, E., Escobar Galindo, R., Sánchez, O., Albella, JM.: Surface and Coatings Technology, vol. 200, 2006, p. 6047

[6] ISO 20502: 2005, Fine ceramics (advanced ceramics, advanced technical ceramics) – Determination of adhesion of ceramic coatings by scratch testing.
[7] Zhang, GA., Yan, PX., Wang, P., Chen, YM., Zhang, JY.: Materials Science and Enineering A, vol. 460–461, 2007, p. 301
[8] Novák M., Lofaj F., Hviščová P.: Key Engineering materials in Local Mechanical Properties 2013, 2014 In press
[9] EN ISO 14577-1: 2002, Metallic materials – Instrumented indentation test for hardness and materials parameters – Part 1: Test method
[10] Kusý, M. – unpublished work
[11] Lin, J., Wu, ZL., Zhang, XH., Mishra, B., Moore, JJ., Sproul, WD.: Thin Solid Films, vol. 517, 2009, p. 1887
[12] Webelements.com
[13] Daniel, R.. Martinschitz, KJ., Keckes, J., Mitterer, C.: Acta Materialia, vol. 58, 2010, p. 2621
[14] Novák, M., Lofaj, F., Hviščová, P.: Powder metalurgy progress, vol. 3, 2013, in press
[15] Kim, SK., Cha, BC.: Surface and Coatings Technology, vol. 188–189, 2004, p. 174
[16] ASTM C 1624-05: 2005, Standard Test Method for Adhesion Strength and Mechanical Failure Modes of Ceramic Coatings by Quantitative Single Point Scratch Testing
[17] Seok, JW., Jadeed, NM., Lin, RY.: Surface and coatings technology, vol. 138, 2001, p. 14
[18] Pauleau, Y.: Vacuum, vol. 61, 2001, p. 175
[19] Freund, LB., Suresh, S. In: Thin film materials. Chapter 2. Cambrige : Cambrige university press., 2009, p. 93
[20] Harper, CA. In: Handbook of ceramics, glasses and diamonds. Chapter 1. New York : McGrawHill Editorial., 2001, p. 42